SOFIE Calibration Product Summary

Mark Hervig, GATS Inc., m.e.hervig@gats-inc.com, 208-354-3315.

Revisions			
Rev.	**Description of Change**	**By**	**Date**
1.0	Draft/Initial version	E. Thompson	2/8/2008
1.1		Mark Hervig	4/21/2008
1.2	Corrected and improved section 4 (Science FOV)	Greg Paxton, Earl Thompson, John Burton, Marty McHugh	5/24/2008
1.3	Added additional descriptions to section 4 following a review of the data	Earl Thompson	5/30/2008
1.4	Updated Section 3 and 4 with the most recent boresight analysis	Greg Paxton	9/8/2008
1.5	added V1.3 FOV data	Mark Hervig	10/28/2009
1.6	added sun sensor RSR	Mark Hervig	1/4/2010
1.7	Updated table 1 along with sections 3 and 7	Greg Paxton	11/5/2010
1.8	Updated boresight, FOV offsets, FOVs, added section 8	Mark Hervig	1/11/2011

This document summarizes the SOFIE calibration results used in ground data processing, and tracks the various products by version number. The SOFIE data processing software uses the individual calibration results described below. The level1 and level2 output files include a single calibration version number ("data processing calibration version"). Table 1 identifies the individual calibration products that are associated with the data processing calibration version.

Calibration data files are at GATS central in: /users/sofie/local/calibration/…

Table 1. SOFIE data processing calibration version tracking.							
Version L1 / L2	**1.01**	**1.02**	**1.022**	**1.03**	**1.2**	**1.3**	**1.4**
Cal product	**Calibration Version**						
Background (Table 2)	1.2	1.2	1.2	1.2			
FOV response functions	1.1	N/A	N/A	1.3	1.4m	1.4m	
Band 3 – sun sensor boresight position	1.0	1.4	1.4	1.4			
FOV offsets (Table 3)	-	-	1.2	1.4			
RSR	1.3	1.3	1.3	1.3: B5-16 1.1: B1-4	1.3: B5-16 1.1: B1-4	1.3 1.1: B1	
Sun sensor RSR	-	-	-	1.1			
ΔV gain (Table 4)	1.1	1.1	1.1	1.1			
Nonlinearity (Table 5)	1.0	1.0	1.0	1.1	1.1?	1.1?	1.2

1. Background

The background (dark current) signal is taken as the measured response from the 16 radiometers when no radiation is entering the telescope aperture. See Table 2 for results.

Version 1.0.

The background was characterized in the lab, as the measured response with the vacuum chamber door closed and the SOFIE door open. These values are based on data collected in November 2006 (data files: vcdus_2006_310_15_52_27_SC.txt and vcdus_2006_310_15_53_31_SC.txt).

Version 1.1.

On-orbit measurements with the telescope door closed on 14 May 2007.

Version 1.2.

Values calculated for each event using detector readings when the FOV is pointed into cold space.

Table 2. SOFIE background signals.

Band	V1.0 (counts)	V1.1 (counts)	
1	15.5	16.4	
2	12.4	13.2	
3	15.9	15.7	
4	13.4	13.6	
5	17.4	17.6	
6	16.3	16.6	
7	17.7	17.5	
8	16.4	16.2	
9	19.2	19.3	
10	18.9	19.3	
11	19.2	18.5	
12	18.6	18.8	
13	14.9	13.4	
14	15.6	15.2	
15	11.6	11.4	
16	15.4	13.8	

2. Field of View (FOV) Response Functions

The relative spatial response of the FOV was characterized in the lab using a variety of techniques and radiative sources. The results yield the FOV response versus angle, in both azimuth and elevation.

All FOV data files are at GATS central in /users/sofie/local/calibration/fov/data_final/.

Version 1.0.

The bands 1 and 2 FOV curves are from knife edge (KE) tests using a xenon lamp as the source. The light was passed through the MIC1 rectangular aperture and scanned vertically through the SOFIE FOV. The resulting FOV curves are the result of a de-convolution of the measured response versus angle and the source intensity versus angle. The bands 3-16 FOV curves are from point source mapping with the solar simulator blackbody as the source. The point source was directed through the MIC1 and stepped through a grid in azimuth and elevation. Because the point source was large, the data were de-convolved with the MIC1 source distribution to derive the FOV curves. *Positive angles are towards space*, negative towards Earth.

All FOV curves are located in angle relative to the band 3 boresight (the band 3 boresight is at zero), and on a uniform angle spacing.

Version 1.1.

This is the V1.0 data with some updates in the processing. The main change was the removal of false off-axis FOV response. *Positive angles are towards space*, negative towards Earth.

Version 1.1a.

This is the V1.1 data with *negative angles towards space*.

Version 1.2.

This is the V1.1 data with the angle scale reversed so that *negative angles are towards space* and positive towards Earth.

Version 1.3.

This is the V1.1 data with off-axis response appended out to -30 and +30 arcmin. The off-axis response was derived using on-orbit solar scans (event 646), which were fit by combining the V1.1 FOVs with adjusted off-axis FOV response from the lab. Mark Hervig did this analysis. *Positive angles are towards space.*

Version 1.4. (from on-orbit solar scans)

Results derived from on-orbit solar scans. FOV main lobes were derived from FFT de-convolution of solar scans and the Allen curve. Wings were appended. All FOVs are located with the weighted centers at zero elevation. Positive angles are towards space. There are 2 sub-versions, V1.4mod had the power in the wings reduced smoothly out to the edges, V1.4trunc was just cutoff past -2 or 2 arcmin.

3. Field of View Boresight Offset

The FOV boresight positions, B(i), for each band, i, are given relative to band 3. The boresight offsets, $\Delta B(i)$, were determined as $\Delta B(i) = B(i) - B(3)$. See Table 3 for results.

Version 1.0.

FOV boresight position was determined as the average of the half-power points. Positive angles are towards space, negative towards Earth.

Version 1.1.

FOV boresight position was determined as the weighted centers (i.e., FOV integral 50% points). Positive angles are towards space, negative towards Earth.

Version 1.2.

FOV boresight position was determined on-orbit as average centers (i.e., average of right and left sides of FOV curve above a certain tolerance during the cruciform calibration). Positive angles are towards space, negative towards Earth. (Refer to section 4.4 for details)

The analysis showed significant differences in band offsets between sunrise (SR) and sunset (SS). Therefore, the offsets were split into SR and SS instead of using one set of offsets for both. Figure 3.1 shows the differences in offset between SR and SS using data for October 2007 and April 2008.

Version 1.3.

Only bands 7 and 13 are corrected to ensure that the offsets are taken into account before altitude registration. Differences in CO_2 band offsets will affect the initial CO_2 altitude registration. Also, previous calibration values were rounded. V1.3 does not use the rounded values.

Version 1.4. (from on-orbit solar scans)

The boresight of each channel was determined as described for band 3 in section 4 for V1.5 results. The boresight offsets reported here are the value for each band minus the band 3 value. The results (Table 3b) are based on event 35569 for sunrise and event 35570 for sunset.

Table 3. SOFIE FOV Boresight Offset Relative to Band 3. All values in arcmin.								
Band	**V1.0**	**V1.1**	**V1.2**		**V1.3**		**V1.4**	
			SS	**SR**	**SS**	**SR**	**SS**	**SR**
1	-0.03	-0.06	-0.009	-0.013	0.0	0.0	-0.030	-0.007
2	-0.01	-0.04	0.0	0.0	0.0	0.0	0.004	0.003
3	0.00	0.00	0.0	0.0	0.0	0.0	0.000	0.000
4	0.00	0.00	-0.056	-0.051	0.0	0.0	-0.041	-0.039
5	-0.21	-0.22	-0.354	-0.19	0.0	0.0	-0.420	-0.314
6	-0.25	-0.23	-0.19	-0.09	0.0	0.0	-0.241	-0.142
7	-0.26	-0.25	-0.091	-0.017	-0.091	-0.017	-0.120	-0.034
8	-0.28	-0.27	-0.07	-0.017	0.0	0.0	-0.067	0.009
9	-0.23	-0.20	-0.218	-0.088	0.0	0.0	-0.281	-0.187
10	-0.28	-0.26	-0.179	-0.05	0.0	0.0	-0.206	-0.102
11	-0.12	-0.15	-0.021	0.0	0.0	0.0	-0.034	0.007
12	-0.16	-0.15	0.004	0.043	0.0	0.0	0.024	0.067
13	0.11	0.10	0.032	0.004	0.032	0.004	0.084	0.006
14	0.05	0.04	0.085	0.071	0.0	0.0	0.067	0.009
15	-0.06	-0.07	0.002	0.05	0.0	0.0	-0.040	-0.042
16	0.23	0.21	0.078	0.027	0.0	0.0	0.130	-0.017

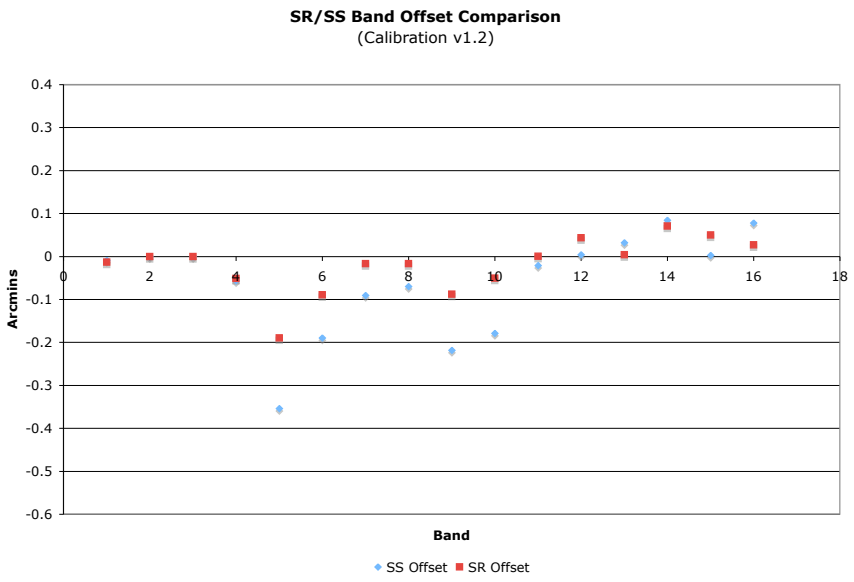

Figure 3.1. Comparison of boresight offsets for sunrise and sunset for V1.2 results.

4. Science FOV (band 3) – Sun Sensor Boresight

The alignment between the science channel detector FOVs and the sun sensor (SS) focal plane array (FPA) is critical when determining the science FOV location on the solar image based on sun sensor data. The SS FPA is 1024 x 1024 pixels covering 2 x 2 degrees. The location of the FOV for band 3 determined by these analyses is used as a reference location for the other band's FOV locations; the locations of the other band's FOVs are measured from the location of Band 3's FOV. After reviewing the various results in May 2008, Version 1.2 was determined to be the best measurement and will likely be used in the 2nd public release.

Version 1.0. (Lab)

Lab results. The solar emulator blackbody (SEB) was directed through the MIC1 collimator and into the SOFIE aperture. The beam was located such that the peak in SOFIE response was obtained, by moving the beam with the MIC1 mirror. The MIC1 aperture was then imaged using the FPA with extended integration time. Because the SEB source only weakly illuminated the FPA, the images were taken at a decimated 8 times factor. These measurements have a fair amount of uncertainty and subsequent measurements (described below) should be used instead of these.

Elevation boresight: pixel 632 (-15 arcmin from FPA center)
Azimuth boresight: pixel 528 (+2 arcmin from FPA center)

Version 1.1. (On-orbit Boresight Calibration)

On-orbit results from Greg Paxton. The SOFIE FOV was scanned across the solar disc in azimuth and elevation (boresight calibration). The operations team used this boresight calibration data to find the elevation and azimuth positions at the maximum FOV intensity location. (This assumes that the maximum FOV intensity is at the center of the sun.) This involves aligning the detector with azimuth and elevation for each scan and selecting the azimuth and elevation pixel location for when the detector value is at its maximum in Excel. Caveat: This analysis did not account for the 0.1 second delay in the detector data due to the electronic filter. Caveat: There is also an issue with how the azimuth edges are determined that could lead to erroneous azimuth edge location values when there is significant slew in the azimuth direction. The right azimuth edge is determined 0.01 seconds before the left azimuth edge, and then another 0.04 seconds elapses before the right azimuth edge is determine again. This problem could be contributing to the Azimuth pixel value of 501.75.

Elevation boresight: pixel 636.16
Azimuth boresight: pixel 501.75

Version 1.2. (On-orbit Cruciform Calibration)

On-orbit results from Greg Paxton. Using the SOFIE cruciform calibration data from multiple events, the operations team found the elevation and azimuth positions at the maximum FOV intensity. The difference between this method and the one used for v1.1 was that the boresight calibration scanned at a much higher slew rate over a larger area (52 arcmin square). The cruciform calibration scans at a much slower slew rate over a smaller area (2 arcmin square).

The slower scans over a smaller area ensured the most accurate solar pointing data. This used a visual method and single events in Excel. Caveat: This analysis did not account for the 0.1 second delay in the detector data due to the electronic filter. After a review of Versions 1.1-1.3 data in May of 2008, Version 1.2 was deemed the best choice. This was substantiated by altitude registration technique comparisons of registrations performed using band 7 and band 13 compared to refraction registration. Version 1.2 data is planned for use in the 2nd public release.

Elevation boresight: pixel 636.15625
Azimuth boresight: pixel 518.46875

Version 1.3. (On-orbit Cruciform Calibration)

On-orbit results from Greg Paxton. Using the SOFIE cruciform calibration data from multiple events, the operations team statistically averaged the FOV boresight from multiple events. In each event, the azimuth and elevation scan portions of the cruciform calibration data were separated into individual arrays. The pixel position for the maximum detector value was recorded by incrementing a pixel count value. After running multiple events, the boresight was selected from the pixel value containing the highest count. Caveat: This analysis did not account for the 0.1 second delay in the detector data due to the electronic filter.

This version was used in the 1st public release of SOFIE data; though the results do agree with the lab measurements (Version 1.0), there is a substantial amount of uncertainty.

Elevation boresight: pixel 632
Azimuth boresight: pixel 528

Version 1.4. (On-orbit Cruciform Calibration)

On-orbit results from Greg Paxton. Using the SOFIE cruciform calibration data from multiple events, the operations team statistically averaged the FOV boresight from multiple events. In each event, the average FOV center between the left and right sides of the curve were calculated utilizing the elevation portion of the cruciform. Figure 4.1 shows that at the 99.9% point of the maximum signal intensity is where the left and right sides of the curve are taken. The left and right points are then averaged to find the calculated intensity center and the elevation position at that center.

The analysis showed that there was a difference of 1 pixel row between SR and SS. Therefore, the SR and SS boresights were split into 2 instead of using one for both. The azimuth position remains unchanged from version 1.2.

SS Elevation boresight: pixel 639.599668
SS Azimuth boresight: pixel 518.46875

SR Elevation boresight: pixel 638.478498
SR Azimuth boresight: pixel 518.46875

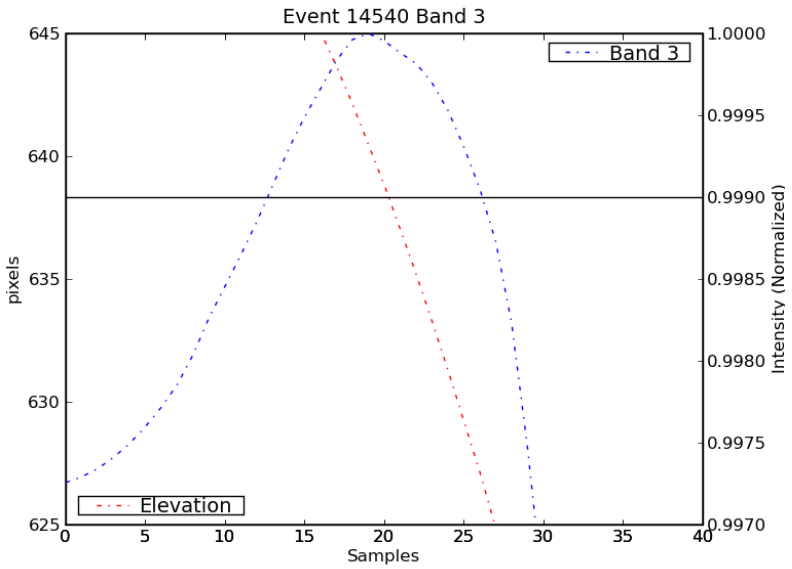

Figure 4.1 Boresight for Event 14540.

Version 1.5. (from on-orbit solar scans, Hervig & Paxton)

The boresight of band 3 was adjusted in elevation such that the response measured during solar scans matched for the space (positive elevation) and Earth sides of the scan. The analysis began with elevations determined using the V1.4 boresight values (above), and the changes determined for V1.5 are adjustments to V1.4. An example of the results is shown in Figure 4.2. Note that adjusting the boresight in elevation produces a symmetric solar scan, as would be expected. The fitting procedure was restricted to ±8 arcmin from sun center where the effect of possible FOV asymmetries (differences between earth and space side FOV response) should be negligible. This analysis did not alter the azimuth boresight position from the V1.4 values. The results below are based on event 35569 for SR and event 35570 for SS.

Note the adjustments determined were a change in the elevation scale of -0.5515 arcmin (-4.608 pixels) for SS and -0.6463 arcmin (-5.401 pixels) for SR. Conversion from arcmin to pixels assumed 7.18 arcsec per pixel in elevation.

SS Elevation boresight: pixel 634.992 (= 639.600 - 4.608)
SS Azimuth boresight: pixel 518.469

SR Elevation boresight: pixel 633.077 (= 638.478 - 5.401)
SR Azimuth boresight: pixel 518.469

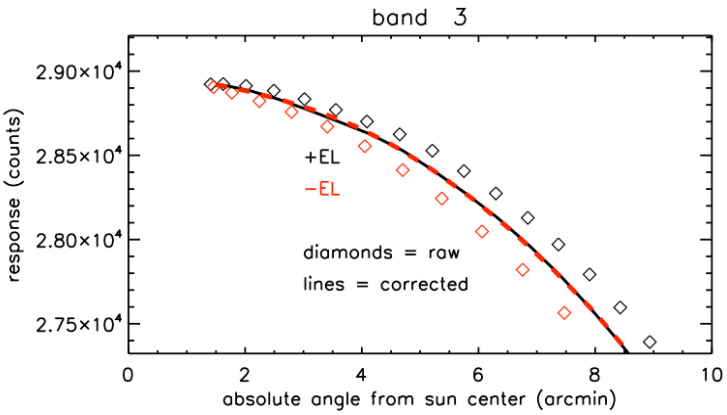

Figure 4.2. SOFIE band 3 response for sunset event 35496, for using the V1.4 boresight (diamonds), and for using the V1.5 boresight (lines).

5. Relative Spectral Response (RSR)

End-to-end RSR calibration was conducted in the lab. The results yield RSR curves that characterize both the in-band and out-of-band RSR. The in-band data are used to characterize the band center wavelengths, defined as mid-way between the half-power points. All raw data were processed by Scott Hanson of SDL (Scott.Hansen@sdl.usu.edu), post processing by Mark Hervig.
All RSR data files are at GATS central in /users/sofie/local/calibration/rsr/data/data_final/.

Version 1.0.

All data at -20°C (nominal temperature). Bands 1-13: Scott Hanson's June 24, 2006 processing of data collected in October 2005. Bands 15-16: Scott Hanson's February 9, 2007 processing of data from the November 2006 calibration combined with earlier data. Note that the bands 1 and 2 out of band response were based on component measurements. The data from Hanson were put on a uniform 2 cm^{-1} spacing for bands 3-16 and a 5 cm^{-1} spacing for bands 1-2. The output files cover the wavelength region defined by the furthest positions where the RSR was greater than 0.001.

Version 1.1.

These results are the V1.0 RSR curves multiplied by the solar spectrum and then re-normalized. The solar spectrum used was from Bob Kurucz, Harvard-Smithsonian Astrophysical Institution, Cambridge, Mass., 617-495-7429.

Version 1.2.

The same as version 1.0, except the wavelength axis goes from band center – 1.5*bandwidth to band center + 1.5*bandwidth.

Version 1.3.

These results are the V1.2 RSR curves multiplied by the solar spectrum and then re-normalized. The solar spectrum used was from Bob Kurucz, Harvard-Smithsonian Astrophysical Institution, Cambridge, Mass., 617-495-7429.

5.1. Sun Sensor Relative Spectral Response (RSR)

The Sun Sensor end-to-end RSR was not measured directly, but rather was determined by combining the measured RSR of the individual optical components (STAR 1000 detector, ND filter, and bandpass filter).

All RSR data files are at GATS central in
/users/sofie/local/calibration/rsr/data/data_final/.

Version 1.0.

These results are based on the STAR 1000 FPA RSR data from the standard spec sheet (the points were taken from the plot on pg. 9), and the measured ND filter and bandpass filter RSR. The RSR curve spans 13700 to14923 1/cm.

Version 1.1

This is the version 1.0 RSR curve multiplied by the solar spectrum and then re-normalized. The solar spectrum used was from Bob Kurucz, Harvard-Smithsonian Astrophysical Institution, Cambridge, Mass., 617-495-7429.

6. Difference Signal Gain

The difference signal gains ($G_{\Delta V}$) were set electronically to specified values. $G_{\Delta V}$ was characterized in the lab using weak band, strong band, and ΔV measurements,

$$G_{\Delta V} = \Delta V / (V_W - V_S) \quad (1)$$

See Table 4 for results.

Version 1.0.

Values specified by design.

Version 1.1.

Measurements in the lab on November 6, 2006 (lab data file: vcdus_2006_310_22_27_33_SC.txt).

Version 1.2.

Measurements on-orbit, analysis by Greg Paxton and Kelly Teague, using events 2896 – 5456.

Table 4. SOFIE difference signal gain calibration results.

Channel	$G_{\Delta V}$ Version 1.0	$G_{\Delta V}$ Version 1.1	$G_{\Delta V}$ Version 1.2	
1	30	30.0	29.80	
2	300	302.8	297.33	
3	96	96.7	96.29	
4	110	109.8	110.39	
5	120	120.1	121.08	
6	202	202.8	202.66	
7	110	110.6	109.65	
8	300	299.9	296.84	

7. Nonlinearity

All indications were that bands 1-4 have a linear response, while bands 5-16 were nonlinear. The nonlinear response in bands 5-16 was calibrated using the small attenuator approach in the lab. The measured nonlinear SOFIE signals (N_M) are corrected to yield a linear response (N_L) by

$$N_L = N_M / f_{NL}(N_M) \quad (2)$$

where $f_{NL}(N_M)$ is the nonlinear term:

$$f_{NL}(N_M) = 1 - K\, N_M\, G_{A,cal} / G_A \quad (3)$$

and K is the nonlinearity constant, G_A is the balance attenuator setting for the given measurement, and $G_{A,cal}$ is the balance attenuator setting used during the lab calibration. In all lab results $G_{A,cal}$ was 0.83. See Table 5 for results.

Version 1.0.

Small attenuator tests in the lab in October 2005, using the SEB as a source. These data were collected with the SOFIE flight ND filter absent and thus covered the complete dynamic range.

Table 5. Nonlinearity constants, K, (10^{-6} counts^{-1}) ± uncertainty (%).

Band	V1.0	V1.1	V1.2
1	0	0	0
2	0	0	0
3	0	0	0
4	0	0	0
5	1.79 ± 5.4	1.79	1.82 ± 1.5
6	1.56 ± 5.8	1.56	1.54 ± 1.7
7	9.58 ± 0.7	9.39	9.29 ± 0.3
8	8.55 ± 1.3	8.55	8.28 ± 0.3
9	0.80 ± 8.2	0.8	0.65 ± 3.8
10	1.60 ± 4.5	1.6	1.54 ± 1.5
11	1.74 ± 3.6	1.74	1.47 ± 1.6
12	2.56 ± 2.8	2.56	2.28 ± 1.1
13	5.01 ± 2.2	5.2	4.37 ± 0.7
14	3.15 ± 2.7	3.15	2.62 ± 1.2
15	1.93 ± 2.8	1.93	1.28 ± 2.4
16	2.20 ± 2.7	2.2	1.52 ± 2.2

Version 1.1.

From analysis of simultaneous retrievals of CO_2 and temperature, Lance had better agreement between the two channels (bands 7 and 13) when he adjusted the non-linearity coefficients for these bands. Further studies will be completed and these values could change slightly.

Version 1.2

Analysis using 4 calibration runs (dates: 2005299, 205307, 2005308, 2006040), with rejection of outliers (2 sigma). Re-processing in Dec 2018.

8. Solar Source Model Wavelength

Analysis of on-orbit solar scans reveals that the Allen curve for the known SOFIE band center wavelength does not match the SOFIE observations. Excellent agreement with SOFIE can be obtained by adjusting the wavelengths used in the Allen formulation (see example in Figure 8.1). This does not imply that the SOFIE band locations are wrong, but rather that the Allen model needs some adjusting that happens to be captured by changing the wavelengths. These wavelengths are given in Table 6.

V1.0: An average of results from events 35496, 35569, and 35570.

Table 6. Best wavelength for Allen model.

Band	SOFIE band center wavelength, from RSR curves (microns)	V1.0 Best wavelength for Allen model (microns)
1	0.292	0.277 ± 1.0%
2	0.330	0.313 ± 0.4%
3	0.867	0.774 ± 0.9%
4	1.037	0.858 ± 1.5%
5	2.462	1.507 ± 0.8%
6	2.618	1.891 ± 0.9%
7	2.785	1.751 ± 0.8%
8	2.939	1.854 ± 1.0%
9	3.064	2.037 ± 0.1%
10	3.186	2.066 ± 0.8%
11	3.384	2.356 ± 1.5%
12	3.479	2.338 ± 2.0%
13	4.324	2.849 ± 3.6%
14	4.646	3.080 ± 4.9%
15	5.006	3.084 ± 3.8%
16	5.316	3.461 ± 3.0%

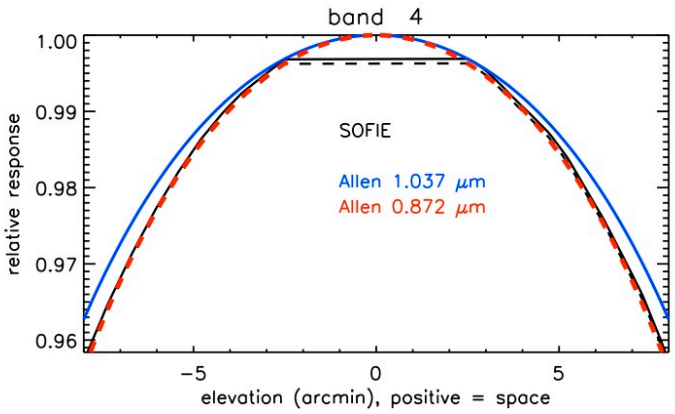

Figure 8.1. SOFIE band 4 response for solar scan during event 35496. The data are compared to Allen curves for the SOFIE wavelength (1.037 μm), and the wavelength which gives the best-match Allen curve (0.872 μm).